Published in final edited form as:
Arthritis Rheumatol. 2014 June ; 66(6): 1648–1658. doi:10.1002/art.38409.

Epigenome-wide scan identifies a treatment-responsive pattern of altered DNA methylation among cytoskeletal remodeling genes in monocytes and CD4+ T cells in Behçet's disease

Travis Hughes[1], **Filiz Ture-Ozdemir**[2], **Fatma Alibaz-Oner**[2], **Patrick Coit**[1], **Haner Direskeneli**[2], and **Amr H Sawalha**[1,3]

[1]Division of Rheumatology, Department of Internal Medicine, University of Michigan, Ann Arbor, MI

[2]Department of Rheumatology, Marmara University, School of Medicine, Istanbul, Turkey

[3]Center for Computational Medicine and Bioinformatics, University of Michigan, Ann Arbor, MI

Abstract

Objective—Behçet's disease (BD) is an inflammatory disease characterized by multi-system involvement including recurrent oral and genital ulcers, cutaneous lesions, and uveitis. The pathogenesis of BD remains poorly understood. We performed a genome-wide DNA methylation study in BD before and after disease remission, and in healthy matched controls.

Methods—We examined genome-wide DNA methylation in monocytes and CD4+ T cells from a set of 16 untreated male BD patients and age, sex, and ethnicity-matched controls. Additional samples were collected from 12 of the same BD patients after treatment and disease remission. Genome-wide DNA methylation patterns were assessed using the HumanMethylation450 DNA Analysis BeadChip array which includes over 485,000 individual methylation sites across the genome.

Results—We identified 383 differentially methylated CpG sites between BD patients and controls in monocytes and 125 differentially methylated CpG sites in CD4+ T cells. Bioinformatic analysis revealed a pattern of aberrant DNA methylation among genes that regulate cytoskeletal dynamics suggesting that aberrant DNA methylation of multiple classes of structural and regulatory proteins of the cytoskeleton might contribute to the pathogenesis of BD. Further, DNA methylation changes associated with treatment act to restore methylation differences observed between patients and controls. Indeed, among CpG sites differentially methylated before and after disease remission, there was almost exclusive reversal of the direction of aberrant DNA methylation observed between patients and healthy controls.

Conclusions—We performed the first epigenome-wide study in BD and provide strong evidence that epigenetic modification of cytoskeletal dynamics underlies the pathogenesis and therapeutic response in BD.

Please address correspondence to Amr H. Sawalha, MD; 5520 MSRB-1, SPC 5680, 1150 W. Medical Center Drive, Ann Arbor, MI 48109, USA. Phone: (734) 763-1858. Fax: (734) 763-4151. asawalha@umich.edu.

Conflict of interest: The authors have no relevant conflicts of interest to disclose.

Keywords

Behçet's Disease; Cytoskeleton; Epigenetics; DNA Methylation

Introduction

Behçet's Disease (BD) is an inflammatory disease characterized by the presence of recurrent oral and genital ulcers, skin lesions, and uveitis. Mucocutaneous lesions in BD are characterized by leukocyte infiltration, primarily by T cells and monocytes (1). Widespread enhancement of leukocyte motility and tissue infiltration is observed in BD. Monocytes from patients with BD display increased activity and promote increased neutrophil adhesion (2). Further, elevated levels of macrophage inflammatory protein 1-alpha, which promotes lymphocyte chemotaxis, are observed in BD (3). Activated CD4+ T cells play a critical role in the pathogenesis of BD, and an expansion of Th17 cells via IL-21 signaling and increased levels of gamma-delta T cells are observed (4–6).

Endothelial cell injury is commonly observed in BD. Elevated levels of soluble E-selectin molecules are observed in serum from BD patients with active disease (7). Impaired function of vascular endothelial cells occurs in response to oxidative damage (8). Disruption of tight junctions between endothelial cells is mediated by changes in class II myosin phosphorylation and remodeling of the F-actin cytoskeleton (9). Cytoskeletal remodeling in endothelial and immune cells accompanies lymphocyte adhesion and tissue infiltration in the normal inflammatory response (10). Treatments that disrupt microtubule processing might be effective in limiting the frequency and severity of mucocutaneous symptoms in BD, but the exact mechanism of action remains uncertain.

There is a strong genetic component to BD evidenced by the geographic concentration of the disease along the Old Silk Road (11). The most robust genetic association observed in BD is within the HLA region. Recent evidence suggests that multiple independent genetic susceptibility loci for BD exist in the HLA class I region, with the most robust effect localized to the genetic region between *HLA-B* and *MICA* genes (12). Multiple associations outside of the HLA region have been reported in BD including *IL10*, *IL23R*, *UBAC2*, *STAT4*, *CCR1*, *KLRC4*, *ERAP1*, and *GIMAP2/GIMAP4* (13). While there is a strong genetic component to BD, genetic variation alone is not sufficient to explain the heritability and pathogenesis of the disease.

The role of DNA methylation in BD has not been explored to date. There is a growing body of evidence supporting an important role for DNA methylation changes in multiple immune-mediated diseases (14–17). DNA methylation refers to the addition of a methyl group to the fifth carbon in cytosine rings within cytosine-guanosine (CpG) dinucleotides. DNA methylation *ex utero* is primarily mediated by DNA methyltransferase 1 (DNMT1) and is generally a repressive epigenetic mark. DNA hypermethylation results in transcriptional gene repression, while hypomethylation is associated with a chromatin configuration that is transcriptionally permissive (18).

Herein, we report results from an epigenome-wide study of the methylation status of over 485,000 individual CpG dinucleotides across the genome among treatment-naïve BD patients and healthy matched controls. We also evaluated epigenome-wide DNA methylation status in the same BD patients before and after treatment and disease remission. We provide evidence for wide-spread DNA methylation changes in BD across the genome. Our data suggest that DNA methylation changes in cytoskeletal dynamics are involved in the pathogenesis of BD and that restoration of DNA methylation of microtubule processing genes is observed following disease remission.

Materials and Methods

Patient Selection and Sample Collection

A total of 16 male BD patients and 16 healthy controls matched for age (+/− 5 years), sex, and ethnicity were recruited to participate in this study. All patients were recruited from the rheumatology clinics at Marmara University in Istanbul, Turkey (Supplementary Table 1). All patients studied had not received prior treatment for BD at least in the previous 3 months, and samples were collected at their initial visit prior to the initiation of treatment. Samples were further collected following treatment and disease remission from 12 of the 16 BD patients included in this study. Disease remission was defined by the absence of any disease-associated symptoms or organ involvement for at least one month. Our study was approved by the ethics committee and the institutional review board at Marmara University and the University of Michigan. All study participants singed a written informed consent prior to participation in this study.

Isolation of Monocytes and CD4+ T cells and DNA extraction

Peripheral blood mononuclear cells (PBMCs) were isolated from fresh blood samples obtained from BD patients and healthy controls using density gradient centrifugation (Amersham Biosciences, Uppsala, Sweden). Monocytes and CD4+ T cells were purified using magnetic bead separation from PBMCs (Miltenyi Biotec, Cologne, Germany). The purity of isolated cell populations was confirmed by flow cytometry analysis using fluorochrome-conjugated antibodies against CD14 for monocytes and CD4 for T-helper lymphocytes and was over 90% for both monocytes and CD4+ T cells. Genomic DNA was obtained from isolated monocytes and CD4+ T cells using the Qiagen DNeasy Blood and Tissue Kit.

Genome-wide DNA Methylation Profiling

Bisulfite conversion was performed using the EZ DNA Methylation Kit (Zymo Research Corp., Irvine, CA, USA). Whole-genome amplification of bisulfite converted DNA was performed prior to array hybridization. The Illumina HumanMethylation450 DNA Analysis BeadChip array was used to assess the methylation status of over 485,000 individual methylation sites throughout the genome. This array covers 99% of RefSeq genes, with an average of 17 CpG sites per gene across the promoter region, 5'-UTR, first exon, gene body, and 3'-UTR. It also covers 96% of CpG islands. Non CpG methylated sites recently identified in human stem cells are also covered as well as microRNA promoter regions.

Quality Control, Identification of Differentially Methylated CpG sites, and Bioinformatic analysis

Comparisons of DNA methylation levels were performed separately among monocytes and CD4+ T cells between BD patients and healthy controls. DNA methylation differences associated with treatment in BD were also separately assessed in monocytes and CD4+ T cells before and after treatment. Differential methylation analysis was performed using the Genome Studio methylation package. Beta values (β) were used to represent percent methylation at each CpG site, which are calculated using the ratio of intensities between methylated and unmethylated alleles as follows:

$$\beta = \frac{Methylated}{Unmethylated + Methylated + 100}$$

Methylation data were normalized in Genome Studio. Prior to analysis a total of 50,446 probes were removed due to the presence of single nucleotide polymorphisms within 10 bases of the CpG target sequence. No probes were observed to have detection p-values greater than 0.05. The *P* value for differential methylation between patients and controls was calculated using the following equation:

$$P = z\left(\frac{|\beta_{patient} - \beta_{control}|}{\frac{s^2_{control}}{N_{control}} - \frac{s^2_{patient}}{N_{patient}}}\right)$$

where *s* is the standard deviation estimate and *z* is the two-sided tail probability of the standard normal distribution. The standard deviation estimate *s* is a function of β and was calculated by the following:

$$s = A\beta^2 + B\beta + C, where A = -0.1511, B = 0.1444, and C = 0.01646$$

A, B and *C* values were derived by Illumina from repeatedly measuring loci with known methylation fractions ranging from 0 to 1 and fitting a parabola to the standard deviation as a function of β.

A differential methylation scores for each probe was calculated as:

$$DiffScore = 10 * sgn(\beta_{patient} - \beta_{control}) * -\log_{10}(p), \text{where} sgn(i) = \begin{cases} i > 0; & +1 \\ i = 0; & 0 \\ i < 0; & -1 \end{cases}$$

Probes with an average methylation difference (delta β) of at least 10% (case-control) or 5% (case-case before and after treatment) and differential methylation scores of at least 22 (equivalent to differential methylation *P* value ≤ 0.01) after adjusting for multiple testing using the Benjamini and Hochberg false discovery rate of 5%, were considered differentially

methylated. A linear regression model was fitted to estimate batch effect in differentially methylated loci using R, and no batch effect was detected in our study.

We performed bioinformatic analysis to identify canonical pathways and cellular processes enriched among differentially methylated CpG sites through gene ontology (GO) analysis using the Database for Annotation, Visualization, and Integrated Discovery (DAVID) (19). We examined enrichment among OMIM diseases, KEGG pathways, Panther pathways, molecular function (MF), cellular component (CC), and biological process (BP) gene ontology terms among differentially methylated gene sets. A background of all RefSeq genes was selected for gene ontology analysis in DAVID. Network interaction analysis was performed using GeneMANIA (20).

Results

Differences in DNA methylation associated with Behçet's disease

We observed significant differences in DNA methylation between BD patients and healthy controls across the genome (Figure 1A). In monocytes, we observed 383 differentially methylated CpG sites between BD patients and controls in 228 genes, with 129 hypermethylated CpG sites and 254 hypomethylated sites (Table 1 and Supplementary Table 2). In CD4+ T cells we observed 125 differentially methylated CpG sites in 62 genes. Specifically, we detected 67 hypomethylated and 58 hypermethylated CpG sites in CD4+ T cells (Table 2 and Supplementary Table 3). While hypomethylation is more prevalent in monocytes, we observed a high degree of concordance between differential methylation between CD4+ T cells and monocytes. Indeed, 59 of the 125 CpG sites differentially methylated in in CD4+ T cells in BD compared to controls were also differentially methylated in BD monocytes.

Bioinformatic analysis

Bioinformatic analysis revealed an enrichment of genes and pathways associated with cytoskeletal remodeling in monocytes among differentially methylated genes between BD patients and healthy controls. DAVID GO term analysis revealed significant enrichment of genes related to cytoskeletal dynamics and function among the 228 genes differentially methylated in monocytes (Table 3). Specifically, cytoskeletal protein binding (MF: 0008092), actin cytoskeleton (CC:0015629), and M band (CC:0031430) showed the most significant enrichment among genes differentially methylated in monocytes.

Among the 62 differentially methylated genes in CD4+ T cells, the most prominent GO terms are related to antigen processing and presentation and are primarily driven by differential methylation in 3 loci within the HLA class II region (Table 4). Enrichment of genes associated with cytoskeletal processes is also observed in CD4+ T cells, but to a lesser degree than that observed in monocytes. In CD4+ T cells, actin cytoskeleton (CC:0015629), cytoskeletal regulation by Rho GTPase (PANTHER:P00016), and cytoskeletal binding protein (MF:0008092) are all significantly enriched (FDR < 0.20).

Differential methylation of genes associated with cytoskeletal remodeling

The set of differentially methylated CpG sites observed in BD monocytes and CD4+ T cells compared to healthy controls includes genes that are involved in multiple levels of cytoskeletal regulation, structure, and function (Supplementary Tables 4 and 5 and Supplementary Figures 1 and 2). Differential methylation of Rho GTPase genes, that play a central role in regulating actin cytoskeletal remodeling (21), is observed in BD CD4+ T cells. Specifically, *RAC1* displays the highest degree of hypomethylation (cg18404925: Case-beta = 0.106, Control-beta = 0.308) in BD CD4+ T cells. *RAC1* regulates T lymphocyte adhesion via integrin and controls actin cytoskeletal dynamics (22, 23). Hypermethylation of the gene which encodes *RhoJ* was also observed in CD4+ T cells of Behçet's patients. Further, *ARHGAP24*, a Rho GTP-associated protein, was hypermethylated in BD monocytes.

Differential methylation of genes involved in actin processing including *FSCN2*, *BAIAP2L1*, *FILIP1*, *SSH1* was present in BD monocytes. Hypermethylation of *BAIAP2L1* and hypomethylation of *FSCN2* was observed in CD4+ T cells (Figure 1B). *ANK1*, coding for ankyrin 1, is associated with attachment of integral membrane proteins to the actin cytoskeleton and was also hypermethylated in BD monocytes compared to healthy controls.

Altered methylation of non-muscle myosin genes was detected in both monocytes and CD4+ T cells in BD patients compared to controls. We observed hypermethylation of Myosin heavy chain 15 (*MYH15*) in monocytes and CD4+ T cells. In monocytes, we further observed hypomethylation of Myosin 1C, (*MYO1C*) and hypermethylation of *MYO1D* and *MPRIP* (Supplementary Table 4).

Differential methylation of genes encoding microtubule-related proteins is observed in both cell types. Hypomethylation of *TBCD*, *KIF1B*, and *DNAH3* was detected in monocytes, and *TUBB8* was hypermethylated in BD CD4+ T cells compared to controls (Figure 1B). In both monocytes and CD4+ T cells there was significant hypomethylation of multiple CpG sites in *RGS14*, a gene which encodes a micro-tubule associated protein (Supplementary Table 4 and 5) (24).

Treatment alters DNA methylation in microtubule processing genes

Widespread DNA methylation changes were observed between monocytes and CD4+ T cells from untreated BD patients with active disease and samples obtained from the same patients following treatment and disease remission. A lower threshold for DNA methylation differences (delta beta ≥ 0.05) was applied to detect smaller changes in DNA methylation and partial restoration by at least 50% of the DNA methylation changes detected in BD. We detected a total of 1,426 differentially methylated CpG sites in monocytes after treatment, and of these 636 were hypomethylated and 790 were hypermethylated. In CD4+ T cells, a total of 2,044 CpG sites were differentially methylated, with 1,012 hypomethylated and 1,032 hypermethylated following treatment.

Bioinformatic analysis of genes that display differential methylation following treatment in BD patients reveals enrichment of multiple GO terms, including some that are related to microtubules in both cell types (Supplementary Table 6). In monocytes, microtubule

cytoskeleton (CC:0015630), microtubule organizing center (CC:0005815), cytoskeleton organization (BP:0007010), and cytoskeleton (CC:0005856) are enriched. Microtubule cytoskeleton (CC:0015630) was also among the top 20 GO terms in CD4+ T cells following treatment.

Altered methylation of genes associated with microtubule structure and organization is observed in both monocytes and CD4+ T cells following treatment (Supplementary Tables 7 and 8). Hypomethylation of tubulin genes *TUBA3C* and *TUBA3D*, and tubulin polymerizing promoting protein (*TPPP*) was observed in BD after treatment and disease remission. Further, we observed significant alteration of the methylation of kinesin and dynein genes in both monocytes and CD4+ T cells. *KIF2A* was hypermethylated in both monocytes and CD4+ T cells following treatment in BD.

Treatment restores DNA methylation changes in Behçet's disease monocytes and CD4+ T cells

After disease remission, alterations in DNA methylation patterns in BD patients were observed to counteract DNA methylation differences seen between BD patients and healthy controls. Among CpG sites differentially methylated before and after treatment, there was almost exclusive reversal of the direction of aberrant methylation observed between cases and controls (Figure 2A). In a comparison of methylation differences identified between BD patients and healthy controls and those detected between the same BD patients before and after treatment, there were 94 overlapping CpG sites among 69 genes in monocytes and 9 overlapping CpG sites among 7 genes in CD4+ T cells. In both cell types, treatment acts to reverse BD-associated differences in DNA methylation. In 93 of the 94 BD-associated CpG sites that display differences following treatment in BD monocytes, the direction of methylation change is opposite to that observed between BD cases and controls (Figure 2B). In many cases DNA methylation in BD patients was completely restored to levels similar to healthy controls following treatment (Supplementary Table 9).

The effect of treatment on BD-associated CpG sites is more pronounced in monocytes than CD4+ T cells. For example, upon disease remission, restoration of DNA hypomethylation of Tubulin folding Cofactor D, *TBCD*, is observed in monocytes. In addition, methylation of multiple CpG within *TRIM39* that were hypomethylated in BD monocytes was restored following treatment to similar levels observed in healthy controls (Supplementary Table 9).

Discussion

In this first epigenomic study in BD, we provided evidence for wide-spread and reversible patterns of altered DNA methylation in this disease. Of particular interest, epigenetic dysregulation in BD was evident across multiple levels of cytoskeletal organization including actin binding, Rho-GTPase enzymes, motor proteins, and microtubule structure. Cytoskeletal rearrangement is a process involved in locomotion, focal adhesion, and cellular proliferation in leukocytes. Our data suggest that aberrant epigenetic regulation of cytoskeletal remodeling genes in BD might underlie increased leukocyte migration and tissue infiltration central to BD pathogenesis.

Among the differentially methylated genes detected in BD, we showed hypomethylation of cytoskeletal genes implicated in increased chemotaxis in normal lymphocytes and invadopodia formation in cancer. Fascin (*FSCN2*) plays a central role in filopodia formation and potentiates invasive migration of cancer cells (25, 26). We observed hypermethylation of *FSCN2* in BD monocytes and CD4+ T cells. Hypomethylation of *SSH1*, a cofilin-phosphatase which regulates actin filament dynamics of cell migration (27), was observed in BD monocytes, but not CD4+ T cells. In monocytes and CD4+ T cells, we observed hypermethylation of *BAIAP2L1* (IRTKS), which functions in actin bundling and cell migration (28, 29).

In BD CD4+ T cells, *RAC1* displays the highest level of hypomethylation between BD patients and controls. Further, partial restoration of reduced *RAC1* methylation was observed in BD patients after disease remission. Differential methylation of *RAC1* accessory proteins was also detected in BD monocytes including actin regulatory protein *ARHGAP24* which functions to reduce expression of *Rac1* and *Cdc42* in murine podocytes (30). *MPRIP*, which was hypomethylated in BD monocytes, is involved in the formation of actin structures that underlay T cell migration through the activation of RAC1 (31). Following treatment in BD monocytes and CD4 + T cells, we observed hypermethylation of Synaptojanin 2 (*SYNJ2*), a RAC1 effector that regulates clathrin-mediated endocytosis and invadopodia formation (32).

In lymphocytes, myosin motor proteins perform a variety of cellular functions including regulation of the cytoskeleton, projections of the cell surface, and cell membrane processes (e.g. phagocytosis) (33). Myosin light chain phosphorylation influences monocyte migration through the endothelial barrier (34). Class II myosins function in cell motility through regulating actin polymerization in the formation of lamellipodia. MYH9 is involved in abrogation of T cell motility upon antigen recognition and focal adhesion (35). In BD monocytes, we observed hypermethylation of Obscurin (*OBSCN*) and *ANK1*. Obscurin is involved in myofibril organization through its regulation of TC10 (RhoQ) and also interacts with *ANK1*.(36, 37) Myosin heavy chain 15 (*MYH15*) was hypermethylated in BD monocytes and CD4+ T cells. Further, altered methylation of myomesin 2 (*MYOM2*) was observed in BD CD4+ T cells.

Immune complex formation might be involved in the pathogenesis of BD (38). Interestingly, cytoskeletal components are frequent targets of autoimmune complexes in BD, and antibodies recognizing intermediate filaments of the cytoskeleton have been observed (39). Further, auto-antibodies targeting Cofilin-1, tubilin-like, and actin-like self-antigens been observed in a subset of patients (40).

We examined the effect of treatment and disease remission on DNA methylation changes in BD monocytes and CD4+ T cells. Colchicine is commonly used as a first-line treatment for mucocutaneous manifestations of BD and was the primary medication used to manage the disease in the patients included in this study. The effectiveness of colchicine in limiting BD severity is thought to lie in its ability to attenuate leukocyte chemotaxis (41). Colchicine is known to limit cell motility through the disruption of microtubule organization and structure. Consistent with this known effect of colchicine, a number of genes related to microtubule formation and organization are differentially methylated in both monocytes and

CD4+ T cells following treatment. Following treatment, hypermethylation of kinesin family member 2A (*KIF2A*) and hypomethylation of tubulin polymerizing promoting protein (*TPPP*) were observed in monocytes and CD4+ T cells. Interestingly, a deficiency of kinesin 2 results in weakened intercellular adhesion without affecting adherens junction components at the plasma membrane (42). Upregulation of *TPPP* has been reported to induce altered microtubule structure and reduce cell viability (43).

In BD monocytes we observed hypermethylation of tubulin folding cofactor D (*TBCD*) that is reversed upon treatment. Similarly, hypomethylation of *TRIM39* in BD monocytes is also reversed following treatment. A genetic association between *TRIM39*, which encodes is a RING domain-containing E3 ubiquitin ligase, and BD has been previously reported in a Japanese population (44). Of interest, we also detected hypomethylation in *UBAC2* in BD monocytes, which encodes a protein with a ubiquitin-associated domain, suggesting a role for this gene product in ubiquitination pathways. *UBAC2* is a confirmed genetic susceptibility locus in BD and the risk allele in this locus has been shown to be associated with increased *UBAC2* mRNA expression in PBMCs (45). The DNA hypomethylation detected in *UBAC2* is almost completely restored upon disease remission in our patients. Differential methylation in several HLA class II loci was notable primarily in CD4+ T cells in BD. Specifically, hypomethylation across several CpG sites in the *HLA-DRB5* and *HLA-DRB6* was observed. There is currently no strong evidence for a genetic susceptibility locus within the HLA class II in BD, despite evidence for multiple independent susceptibility loci located within the HLA class I (12).

In summary, our data provide evidence for epigenetic remodeling and reversal of specific DNA methylation changes following disease remission in an inflammatory disease. This observation emphasizes the potential for epigenetic studies to uncover novel aspects of disease pathogenesis and therefore the identification of new targets for disease monitoring and treatment. We provide strong evidence that dynamic and reversible epigenetic changes in cytoskeletal remodeling genes might play an important role in the pathogenesis of BD. We report epigenetic remodeling among BD-associated variation in DNA methylation following treatment which acts to reverse DNA methylation differences observed between BD cases and controls (Figure 2). DNA methylation changes restored upon disease remission represent potential biomarkers for disease activity and treatment responsiveness in BD. A large longitudinal study will be necessary to fully explore these altered DNA methylation changes as biomarkers. Future studies to characterize the capacity of specific DNA methylation changes in BD and other inflammatory and autoimmune diseases to predict disease manifestations, clinical course, and response to treatment are warranted.

Supplementary Material

Refer to Web version on PubMed Central for supplementary material.

Acknowledgments

Funding for this project was provided by the Rheumatology Research Foundation's Rheumatology Investigator award and the National Institutes of Health grant number P30ES017885 to A.H.S.

References

1. Müller W, Lehner T. Quantitative electron microscopical analysis of leukocyte infiltration in oral ulcers of Behcet's syndrome. British Journal of Dermatology. 1982; 106(5):535–544. [PubMed: 7073979]
2. Şahln Ş, Lawrence R, Direskeneli H, Hamuryudan V, Yazici H, Akoğlu T. Monocyte activity in Behcet's disease. Rheumatology. 1996; 35(5):424–429.
3. Kim W, Do J, Park K, Cho M, Park S, Cho C, et al. Enhanced production of macrophage inhibitory protein-1alpha in patients with Behcet's disease. Scandinavian journal of rheumatology. 2004; 34(2):129–135. [PubMed: 16095009]
4. Geri G, Terrier B, Rosenzwajg M, Wechsler B, Touzot M, Seilhean D, et al. Critical role of IL-21 in modulating T_H 17 and regulatory T cells in Behçet disease. Journal of Allergy and Clinical Immunology. 2011; 128(3):655–664. [PubMed: 21724243]
5. Suzuki Y, Hoshi K, Matsuda T, Mizushima Y. Increased peripheral blood gamma delta+ T cells and natural killer cells in Behçet's disease. The Journal of Rheumatology. 1992; 19(4):588. [PubMed: 1534375]
6. Parlakgul G, Guney E, Erer B, Kilicaslan Z, Direskeneli H, Gul A, et al. Expression of regulatory receptors on gammadelta T Cells and their cytokine production in Behcet's disease. Arthritis Res Ther. 2013; 15(1):R15. [PubMed: 23336215]
7. Triolo G, Accardo-Palumbo A, Triolo G, Carbone MC, Ferrante A, Giardina E. Enhancement of endothelial cell E-selectin expression by sera from patients with active Behçet's disease: moderate correlation with anti-endothelial cell antibodies and serum myeloperoxidase levels. Clinical Immunology. 1999; 91(3):330–337. [PubMed: 10370379]
8. Niwa Y, Miyake S, Sakane T, Shingu M, Yokoyama M. Auto-oxidative damage in Behcet's disease--endothelial cell damage following the elevated oxygen radicals generated by stimulated neutrophils. Clinical and experimental immunology. 1982; 49(1):247. [PubMed: 7127901]
9. Ivanov AI, McCall IC, Parkos CA, Nusrat A. Role for actin filament turnover and a myosin II motor in cytoskeleton-driven disassembly of the epithelial apical junctional complex. Molecular biology of the cell. 2004; 15(6):2639–2651. [PubMed: 15047870]
10. Ivanov AI, Parkos CA, Nusrat A. Cytoskeletal regulation of epithelial barrier function during inflammation. The American journal of pathology. 2010; 177(2):512–524. [PubMed: 20581053]
11. Verity D, Marr J, Ohno S, Wallace G, Stanford M. Behçet's disease, the Silk Road and HLA-B51: historical and geographical perspectives. Tissue antigens. 1999; 54(3):213–220. [PubMed: 10519357]
12. Hughes T, Coit P, Adler A, Yilmaz V, Aksu K, Duzgun N, et al. Identification of multiple independent susceptibility loci in the HLA region in Behcet's disease. Nat Genet. 2013; 45(3):319–324. [PubMed: 23396137]
13. Gul A. Genetics of Behcet's disease: lessons learned from genomewide association studies. Curr Opin Rheumatol. 2014; 26(1):56–63. [PubMed: 24257369]
14. Coit P, Jeffries M, Altorok N, Dozmorov MG, Koelsch KA, Wren JD, et al. Genome-wide DNA methylation study suggests epigenetic accessibility and transcriptional poising of interferon-regulated genes in naive CD4+ T cells from lupus patients. J Autoimmun. 2013; 43:78–84. [PubMed: 23623029]
15. Altorok N, Coit P, Hughes T, Koelsch KA, Stone DU, Rasmussen A, et al. Genome-wide DNA methylation patterns in naive CD4 T cells from patients with primary Sjogren's syndrome. Arthritis Rheum. 2013
16. de la Rica L, Urquiza JM, Gomez-Cabrero D, Islam AB, Lopez-Bigas N, Tegner J, et al. Identification of novel markers in rheumatoid arthritis through integrated analysis of DNA methylation and microRNA expression. J Autoimmun. 2013; 41:6–16. [PubMed: 23306098]
17. Sunahori K, Nagpal K, Hedrich CM, Mizui M, Fitzgerald LM, Tsokos GC. The catalytic subunit of protein phosphatase 2A (PP2Ac) promotes DNA hypomethylation by suppressing the phosphorylated mitogen-activated protein kinase/extracellular signal-regulated kinase (ERK) kinase (MEK)/phosphorylated ERK/DNMT1 protein pathway in T-cells from controls and

systemic lupus erythematosus patients. J Biol Chem. 2013; 288(30):21936–21944. [PubMed: 23775084]

18. Sawalha AH. Epigenetics and T-cell immunity. Autoimmunity. 2008; 41(4):245–252. [PubMed: 18432405]
19. Da Wei Huang BTS, Lempicki RA. Systematic and integrative analysis of large gene lists using DAVID bioinformatics resources. Nature protocols. 2008; 4(1):44–57.
20. Warde-Farley D, Donaldson SL, Comes O, Zuberi K, Badrawi R, Chao P, et al. The GeneMANIA prediction server: biological network integration for gene prioritization and predicting gene function. Nucleic Acids Res. 2010; 38:W214–W220. (Web Server issue). [PubMed: 20576703]
21. Heasman SJ, Ridley AJ. Mammalian Rho GTPases: new insights into their functions from in vivo studies. Nature reviews Molecular cell biology. 2008; 9(9):690–701.
22. D'Souza-Schorey C, Boettner B, Van Aelst L. Rac regulates integrin-mediated spreading and increased adhesion of T lymphocytes. Molecular and cellular biology. 1998; 18(7):3936–3946. [PubMed: 9632778]
23. Tapon N, Hall A. Rho, Rac and Cdc42 GTPases regulate the organization of the actin cytoskeleton. Current opinion in cell biology. 1997; 9(1):86–92. [PubMed: 9013670]
24. Martin-McCaffrey L, Willard FS, Pajak A, Dagnino L, Siderovski DP, D'Souza SJ. RGS14 is a microtubule-associated protein. Cell Cycle. 2005; 4(7):953–960. [PubMed: 15917656]
25. Li A, Dawson JC, Forero-Vargas M, Spence HJ, Yu X, König I, et al. The actin-bundling protein fascin stabilizes actin in invadopodia and potentiates protrusive invasion. Current Biology. 2010; 20(4):339–345. [PubMed: 20137952]
26. Vignjevic D, Kojima S-i, Aratyn Y, Danciu O, Svitkina T, Borisy GG. Role of fascin in filopodial protrusion. The Journal of cell biology. 2006; 174(6):863–875. [PubMed: 16966425]
27. Huang TY, DerMardirossian C, Bokoch GM. Cofilin phosphatases and regulation of actin dynamics. Current opinion in cell biology. 2006; 18(1):26–31. [PubMed: 16337782]
28. Millard TH, Dawson J, Machesky LM. Characterisation of IRTKS, a novel IRSp53/MIM family actin regulator with distinct filament bundling properties. Journal of cell science. 2007; 120(9): 1663–1672. [PubMed: 17430976]
29. Chen G, Li T, Zhang L, Yi M, Chen F, Wang Z, et al. Src-stimulated IRTKS phosphorylation enhances cell migration. FEBS letters. 2011; 585(19):2972–2978. [PubMed: 21840312]
30. Akilesh S, Suleiman H, Yu H, Stander MC, Lavin P, Gbadegesin R, et al. Arhgap24 inactivates Rac1 in mouse podocytes, and a mutant form is associated with familial focal segmental glomerulosclerosis. The Journal of clinical investigation. 2011; 121(10):4127. [PubMed: 21911940]
31. Sala-Valdés M, Gordón-Alonso M, Tejera E, Ibáñez A, Cabrero JR, Ursa A, et al. Association of syntenin-1 with M-RIP polarizes Rac-1 activation during chemotaxis and immune interactions. Journal of cell science. 2012; 125(5):1235–1246. [PubMed: 22349701]
32. Chuang, Y-y; Tran, NL.; Rusk, N.; Nakada, M.; Berens, ME.; Symons, M. Role of synaptojanin 2 in glioma cell migration and invasion. Cancer research. 2004; 64(22):8271–8275. [PubMed: 15548694]
33. Maravillas-Montero JL, Santos-Argumedo L. The myosin family: unconventional roles of actin-dependent molecular motors in immune cells. Journal of Leukocyte Biology. 2012; 91(1):35–46. [PubMed: 21965174]
34. Haidari M, Zhang W, Chen Z, Ganjehei L, Warier N, Vanderslice P, et al. Myosin light chain phosphorylation facilitates monocyte transendothelial migration by dissociating endothelial adherens junctions. Cardiovascular research. 2011; 92(3):456–465. [PubMed: 21908648]
35. Jacobelli J, Chmura SA, Buxton DB, Davis MM, Krummel MF. A single class II myosin modulates T cell motility and stopping, but not synapse formation. Nature immunology. 2004; 5(5):531–538. [PubMed: 15064761]
36. Coisy-Quivy M, Touzet O, Bourret A, Hipskind RA, Mercier J, Fort P, et al. TC10 controls human myofibril organization and is activated by the sarcomeric RhoGEF obscurin. Journal of cell science. 2009; 122(7):947–956. [PubMed: 19258391]

37. Bagnato P, Barone V, Giacomello E, Rossi D, Sorrentino V. Binding of an ankyrin-1 isoform to obscurin suggests a molecular link between the sarcoplasmic reticulum and myofibrils in striated muscles. The Journal of cell biology. 2003; 160(2):245–253. [PubMed: 12527750]

38. Williams B, Lehner T. Immune complexes in Behçet's syndrome and recurrent oral ulceration. British medical journal. 1977; 1(6073):1387. [PubMed: 324574]

39. Akoğlu T, Kozakoğlu H, Akoğlu E. Antibody to intermediate filaments of the cytoskleton in patients with Behçet's disease. Clinical immunology and immunopathology. 1986; 41(3):427–432. [PubMed: 3780056]

40. Ooka S, Nakano H, Matsuda T, Okamoto K, Suematsu N, Kurokawa MS, et al. Proteomic surveillance of autoantigens in patients with Behçet's disease by a proteomic approach. Microbiology and immunology. 2010; 54(6):354–361. [PubMed: 20536734]

41. Jorizzo JL, Hudson RD, Schmalstieg FC, Daniels JC, Apisarnthanarax P, Henry JC, et al. Behçet's syndrome: immune regulation, circulating immune complexes, neutrophil migration, and colchicine therapy. Journal of the American Academy of Dermatology. 1984; 10(2):205–214. [PubMed: 6371066]

42. Nekrasova OE, Amargo EV, Smith WO, Chen J, Kreitzer GE, Green KJ. Desmosomal cadherins utilize distinct kinesins for assembly into desmosomes. The Journal of cell biology. 2011; 195(7): 1185–1203. [PubMed: 22184201]

43. Lehotzky A, Tirián L, Tökési N, Lénárt P, Szabó B, Kovács J, et al. Dynamic targeting of microtubules by TPPP/p25 affects cell survival. Journal of cell science. 2004; 117(25):6249–6259. [PubMed: 15564385]

44. Kurata R, Nakaoka H, Tajima A, Hosomichi K, Shiina T, Meguro A, et al. TRIM39 and RNF39 are associated with Behçet’s disease independently of HLA-B*51 and -A*26. Biochemical and biophysical research communications. 2010; 401(4): 533–537. [PubMed: 20875797]

45. Sawalha AH, Hughes T, Nadig A, Yilmaz V, Aksu K, Keser G, et al. A putative functional variant within the UBAC2 gene is associated with increased risk of Behcet's disease. Arthritis Rheum. 2011; 63(11):3607–3612. [PubMed: 21918955]

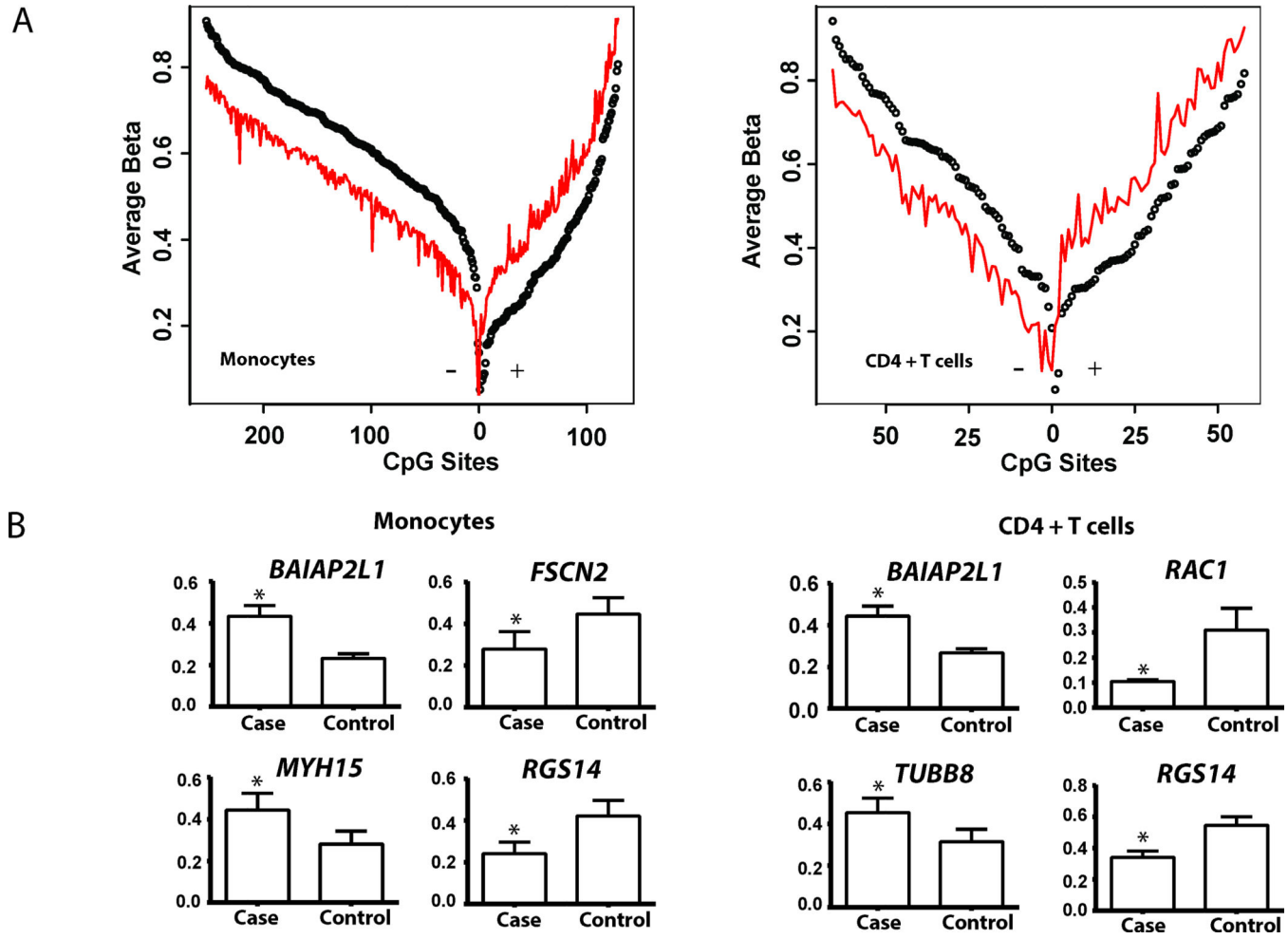

Figure 1. Differential methylation in Behçet's disease monocytes and CD4+ T cells

(A) Differential methylation is observed between 16 male Behçet's disease (BD) cases and 16 age-, sex-, and ethnicity-matched controls. In monocytes, 383 CpG sites were differentially methylated, of which 254 were hypomethylated and 129 were hypermethylated. In CD4+ T cells, 125 differentially methylated CpG sites were observed, 67 of which were hypomethylated and 58 were hypermethylated. Differentially methylated CpG sites are arranged with hypomethylated sites on the left and hypermethylated sites on the right within each panel. For each CpG site the average beta values, which represent percent methylation are shown (red: BD cases, black: controls). The distance between each point and the continuous red line represents the extent of differential methylation (BD Case Methylation – Control Methylation). **(B)** Differential methylation of a number of genes related to cytoskeletal dynamics is observed in BD monocytes and CD4+ T cells. Shown are differences in average methylation between BD cases and matched controls (Mean, SEM).

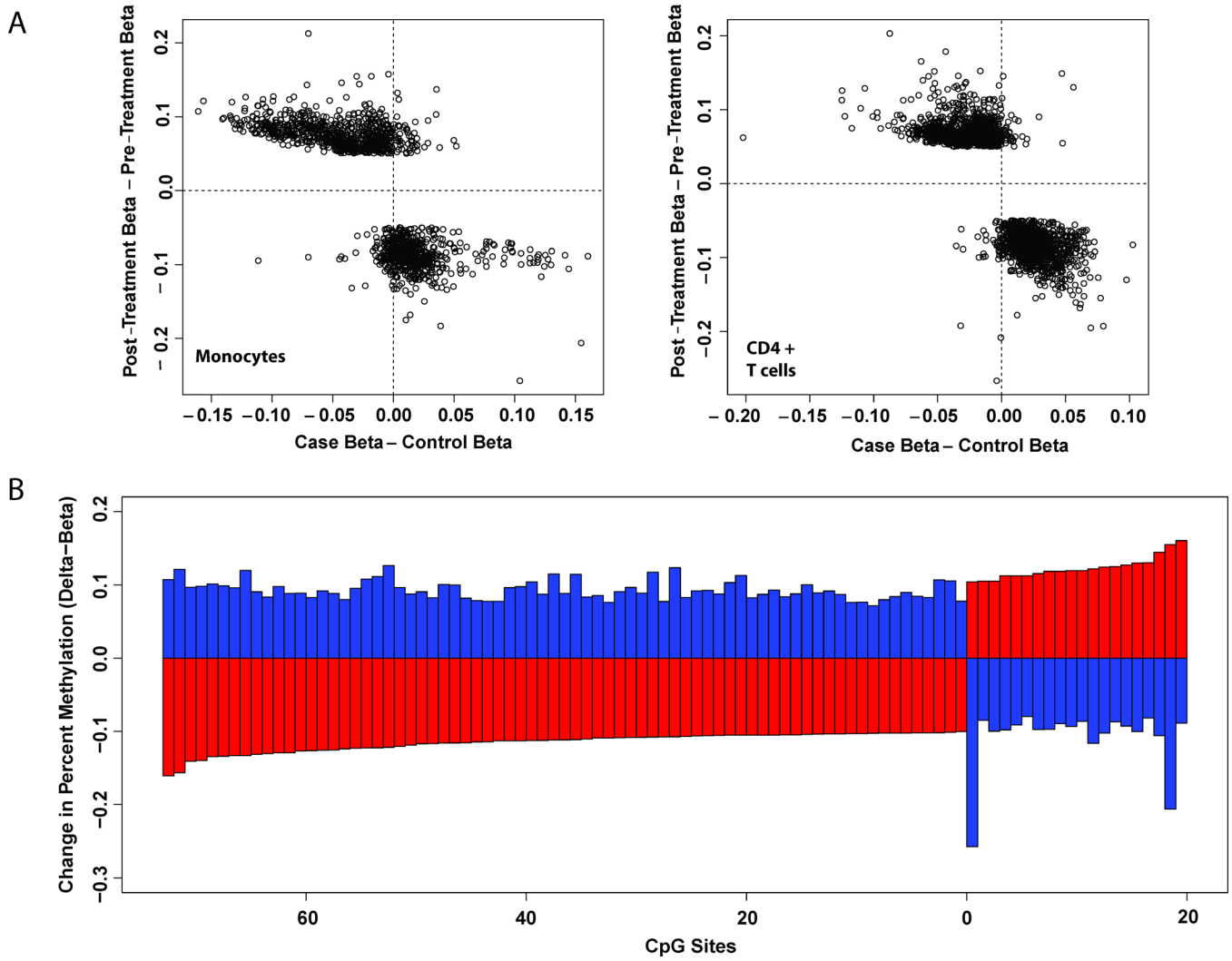

Figure 2. Treatment restores DNA methylation changes in Behçet's disease

(A) CpG sites differentially methylated upon treatment (|Differential score| ≥22, |Delta-beta| ≥ 0.05) are plotted according to differences in DNA methylation observed between BD patients and controls on the x-axis and change in methylation upon treatment on the y axis. CpG sites hypomethylated in BD patients lie to the left of the vertical dotted line, while hypermethylated sites lies to the right. CpG sites with increased and decreased methylation following treatment lie above and below the horizontal dotted line, respectively. CpG sites contained in the upper-left and lower-right quadrants are those in which treatment acts to reverse differences observed between BD cases and controls. Enrichment of treatment-responsive CpGs in the upper-left and lower-right quadrants of the plot demonstrates that treatment acts to reverse BD methylation differences. **(B)** In 93 of the 94 BD-associated differentially methylated CpG sites in monocytes that also display differential methylation in patients following disease remission, the direction of methylation change is opposite to that observed between patients and healthy controls. Red bars represent the difference in percent methylation between patients and controls, while blue bars represent the difference in

percent methylation on the same CpG sites between patients after disease remission compared to the same patients before treatment.

Table 1

Differentially methylated CpG sites in monocytes from BD patients compared to healthy controls. The most differentially hypomethylated and hypermethylated sites are depicted.

Probe	Gene Symbol	Gene Name	Methylation (Beta) Cases	Methylation (Beta) Controls	Delta Beta	*P* value
Hypomethylated						
cg07211972	*CBS*	Cystathionine-beta-synthase	0.374	0.604	−0.230	1.59E-34
cg15971518	*PRG2*	Proteoglycan 2, bone marrow	0.282	0.470	−0.187	6.85E-25
cg17509989	*RGS14*	Regulator of G-protein signaling 14	0.242	0.421	−0.179	5.35E-24
cg16006841	*RGS14*	Regulator of G-protein signaling 14	0.341	0.519	−0.178	4.67E-21
cg06060754	*RGS14*	Regulator of G-protein signaling 14	0.315	0.488	−0.173	3.74E-20
cg05248234	*FSCN2*	Fascin homolog 2, actin-bundling protein, retinal	0.280	0.450	−0.170	2.97E-20
cg06559318	*HLA-DRB6*	Major histocompatibility complex, class II, DR beta 6	0.282	0.444	−0.162	2.85E-18
cg05398700	*WDR20*	WD repeat domain 20	0.644	0.805	−0.161	5.38E-25
cg23646109	*BCYRN1; GJB1*	Brain cytoplasmic RNA 1; gap junction protein, beta 1, 32kDa	0.751	0.907	−0.156	1.59E-34
cg17220055	*HIVEP3*	Human immunodeficiency virus type I enhancer binding protein 3	0.401	0.554	−0.153	7.7E-15
Hypermethylated						
cg08684580	*BAIAP2L1*	BAI1-associated protein 2-like 1	0.434	0.234	0.200	8.89E-35
cg24634471	*JRK*	Jerky homolog (mouse)	0.630	0.434	0.195	8.89E-35
cg10596483	*JRK*	Jerky homolog (mouse)	0.522	0.349	0.172	8.89E-35
cg26053840	*GLO1*	Glyoxalase I	0.465	0.305	0.160	8.89E-35
cg17965159	*LRMP*	Lymphoid-restricted membrane protein	0.594	0.434	0.160	8.89E-35
cg03329597	*MYH15*	Myosin, heavy chain 15	0.442	0.284	0.159	8.89E-35
cg07921503	*CHST12*	Carbohydrate (chondroitin 4) sulfotransferase 12	0.226	0.072	0.155	8.89E-35
cg10105218	*CD53*	CD53 molecule	0.397	0.249	0.149	8.89E-35
cg06915202	*BAIAP2L1*	BAI1-associated protein 2-like 1	0.469	0.321	0.148	8.89E-35
cg14040931	*GNE*	Glucosamine (UDP-N-acetyl)-2-epimerase/N-acetylmannosamine kinase	0.488	0.342	0.146	8.89E-35

Table 2

Differentially methylated CpG sites in CD4+ T cells from BD patients compared to healthy controls. The most differentially hypomethylated and hypermethylated sites are depicted.

Probe	Gene Symbol	Gene name	Methylation (Beta) Cases	Methylation (Beta) Controls	Delta Beta	*P* value
Hypomethylated						
cg18404925	*RAC1*	Cell migration-inducing gene 5 protein	0.106	0.308	−0.202	1.79E-34
cg17509989	*RGS14*	Regulator of G-protein signaling 14	0.343	0.545	−0.201	1.42E-27
cg00103771	*HLA-DRB6*	Major histocompatibility complex, class II, DR beta 6	0.453	0.644	−0.192	3.28E-25
cg06559318	*HLA-DRB6*	Major histocompatibility complex, class II, DR beta 6	0.265	0.448	−0.183	2.85E-24
cg16006841	*RGS14*	Regulator of G-protein signaling 14	0.507	0.678	−0.171	1.02E-20
cg27362989	*HLA-DRB5*	Major histocompatibility complex, class II, DR beta 5	0.322	0.489	−0.167	1.05E-18
cg23646109	*BCYRN1, GJB1*	Brain cytoplasmic RNA 1; gap junction protein, beta 1, 32kDa	0.737	0.897	−0.160	1.79E-34
cg01778345	*GDAP2*	Ganglioside induced differentiation associated protein 2	0.485	0.630	−0.145	1.6E-13
cg19516921	*HLA-DRB5*	Major histocompatibility complex, class II, DR beta 5	0.326	0.470	−0.144	2.08E-13
cg06060754	*RGS14*	Regulator of G-protein signaling 14	0.475	0.612	−0.137	6.29E-12
Hypermethylated						
cg16474696	*MRI1*	Methylthioribose-1-phosphate isomerase 1; mediator of RhoA-dependent invasion	0.430	0.244	0.186	1.02E-34
cg08684580	*BAIAP2L1*	BAI1-associated protein 2-like 1	0.444	0.268	0.176	1.02E-34
cg24634471	*JRK*	Jerky homolog (mouse)	0.564	0.390	0.174	1.02E-34
cg07796016	*LCE1C*	Late cornified envelope 1C	0.755	0.596	0.158	1.02E-34
cg04798314	*SMYD3*	SET and MYND domain containing 3	0.705	0.550	0.155	1.02E-34
cg16913477	*C3orf39*	Chromosome 2 open reading frame	0.898	0.758	0.141	1.02E-34
cg00501169	*NBPF4*	Neuroblastoma breakpoint family, member 4	0.811	0.672	0.139	1.02E-34
cg10596483	*JRK*	Jerky homolog (mouse)	0.485	0.346	0.139	3.39E-12
cg26679884	*TUBB8*	Tubulin, beta 8 class VIII	0.455	0.317	0.138	1.75E-12
cg25755428	*MRI1*	Methylthioribose-1-phosphate isomerase 1; mediator of RhoA-dependent invasion	0.238	0.100	0.138	1.02E-34

Table 3

Gene ontology analysis of differentially methylated CpG sites in monocytes from Behçet's disease patients compared to healthy controls

Category	Description	Genes	*P* Value	FDR (%)
Monocytes				
MF:0008092	Cytoskeletal protein binding	*OBSCN, MYH15, SSH1, MYO1C, FSCN2, BAIAP2L1, BAIAP2, MYO1D, RPH3AL, SYNPO2, HOMER2, TNNI2, MPRIP, KIF1B, ANK1*	0.0024	3.37
CC:0015629	Actin Cytoskeleton	*MYH15, FSCN2, MYO1C, MYO1D, FERMT1, SYNPO2, SLC9A3R1, BMF, FILIP1L, TNNI2*	0.0037	4.75
CC:0031430	M band	*OBSCN, ANK1, ENO1*	0.0044	5.59
CC:0016459	Myosin Complex	*MYH15, MYO1C, MYO1D, BMF, FILIP1L*	0.0064	8.04
CC:0030016	Myofibril	*HDAC4, OBSCN, ANK1, MYH15, TNNI2, ENO1*	0.0088	10.87
MF:0008093	Cytoskeletal adaptor activity	*ANK1, BAIAP2L1, BAIAP2*	0.0097	12.92
CC:0005737	Cytoplasm	*TGOLN2, MYH15, CHMP6, C16ORF70, MIPEP, CUL3, NLRC4, ANK1, EDARADD, BSG, BCL2L14, BAIAP2, HAL, PDE4D, RPTOR, NPC1, ATP2C1, TRIM34, PCMTD1, FILIP1L, ANKFY1, MCTS1, TRIM39, SH3GL1, SSH1, PFKFB3, GNE, CLU, CALR, AZI1, SCRIB, ADAP1, JRK, ARG1, LPCAT1, GALNS, DHODH, RNF11, DYRK4, GLO1, TRAF6, BMF, TEC, B4GALT5, PTPN7, OBSCN, UAP1, ABR, MYO1C, NXF2, RPS9, SULT6B1, HOMER2, MPRIP, TNNI2, HDAC4, LASS3, HIVEP3, COPS2, MAD1L1, FERMT1, IL4I1, CD93, CHST12, TRIM6, CHST15, ACAD8, GOLGA3, PIGY, RPH3AL, ARHGAP24, PRKCB, EML4, EIF4G1, KIF1B, HIPK3, LRMP, GNAS, PCYOX1, TRIM6-TRIM34, SEC14L1, STK40, DAPP1, CCS, ETV6, PCSK6, EXOC2, ENO1, FAM125B, NXF2B, SYNPO2, PARK2, STAB2, CSGALNACT1, MRPL21, RPS6KA2, TRPC4AP, CYP4F3, RAB38, SLC15A4, VPS28, ACSM5, CBS*	0.011	13.81
CC:0043292	Contractile fiber	*HDAC4, OBSCN, ANK1, MYH15, TNNI2, ENO1*	0.012	15.07
CC:0005856	Cytoskeleton	*MAD1L1, MYH15, SSH1, GNE, DNAH3, FERMT1, AZI1, ANK1, BMF, DLG2, FSCN2, MYO1C, MYO1D, NXF2B, NXF2, SYNPO2, PDE4D, SLC9A3R1, ARHGAP24, HOMER2, RGS14, TNNI2, MPRIP, EML4, KIF1B, TBCD, FILIP1L*	0.014	16.44
CC:0031672	A band	*OBSCN, ANK1, ENO1*	0.014	16.72
BP:0009225	Nucleotide-sugar metabolic process	*CSGALNACT1, UAP1, GNE*	0.012	18.04
CC:0005802	Trans-Golgi network k	*TGOLN2, ATP2C1, C16ORF70, GNAS*	0.015	18.32
MF:0003779	Actin binding	*MYH15, SSH1, FSCN2, MYO1C, BAIAP2L1, MYO1D, SYNPO2, HOMER2, TNNI2, MPRIP*	0.015	18.75
CC:0012505	Endomembrane system	*MAD1L1, BSG, BCL2L14, PIGY, MYO1C, CHMP6, C16ORF70, RPH3AL, CSGALNACT1, NPC1, KIF1B, ATP2C1, CHST12, LRMP, GNAS, CYP4F3, GOLGA3*	0.017	19.91

Table 4

Gene ontology analysis of differentially methylated CpG sites in CD4+ T cells from Behçet's disease patients compared to healthy controls

Category	Description	Genes	*P* Value	FDR (%)
KEGG:hsa05310	Asthma	*HLA-DQB1, EPX, PRG2, HLA-DRB5, HLA-DQA1*	8.21E-07	7.42E-04
KEGG:hsa05416	Viral myocarditis	*HLA-DQB1, MYH15, RAC1, HLA-DRB5, HLA-DQA1*	3.14E-05	0.0284
KEGG:hsa04612	Antigen processing and presentation	*HLA-DQB1, HLA-DRB5, NFYA, HLA-DQA1*	0.0013	1.21
CC:0042613	MHC class II protein complex	*HLA-DQB1, HLA-DRB5, HLA-DQA1*	0.0029	3.32
KEGG:hsa05330	Allograft rejection	*HLA-DQB1, HLA-DRB5, HLA-DQA1*	0.0042	3.74
KEGG:hsa05332	Graft-versus-host disease	*HLA-DQB1, HLA-DRB5, HLA-DQA1*	0.0049	4.36
KEGG:hsa04940	Type I diabetes mellitus	*HLA-DQB1, HLA-DRB5, HLA-DQA1*	0.0057	5.03
BP:0002504	Antigen processing and presentation of peptide or polysaccharide antigen via MHC class II	*HLA-DQB1, HLA-DRB5, HLA-DQA1*	0.0043	6.06
KEGG:hsa04672	Intestinal immune network for IgA production	*HLA-DQB1, HLA-DRB5, HLA-DQA1*	0.0077	6.74
CC:0015629	Actin cytoskeleton	*MYH15, FSCN2, MYOM2, FERMT1, TNNI2*	0.0064	7.18
KEGG:hsa05320	Autoimmune thyroid disease	*HLA-DQB1, HLA-DRB5, HLA-DQA1*	0.0083	7.26
OMIM	Celiac disease, susceptibility to	*HLA-DQB1, HLA-DQA1*	0.011	8.60
CC:0043234	Protein complex	*HLA-DQB1, MYH15, TOLLIP, FERMT1, NFYA, HLA-DQA1, GJB1, TNNI2, MYOM2, HLA-DRB5, TUBB8, IFFO1, NCOR2, GOLGA3, GABRP*	0.008	8.90
PANTHER:P00016	Cytoskeletal regulation by Rho GTPase	*RHOJ, MYH15, RAC1, TUBB8*	0.012	9.00
CC:0042611	MHC protein complex	*HLA-DQB1, HLA-DRB5, HLA-DQA1*	0.011	11.90
CC:0032991	Macromolecular complex	*HLA-DQB1, MYH15, TOLLIP, FERMT1, NFYA, HLA-DQA1, GJB1, TNNI2, JRK, MYOM2, HLA-DRB5, TUBB8, IFFO1, GOLGA3, NCOR2, GABRP*	0.019	19.77
MF:0008092	Cytoskeletal protein binding	*MYH15, FSCN2, BAIAP2L1, FRMD4A, RPH3AL, TNNI2*	0.018	19.79